This article has been accepted for publication in a future issue of this journal, but has not been fully edited. Content may change prior to final publication. Citation information: DOI 10.1109/TETC.2016.2555806, IEEE Transactions on Emerging Topics in Computing

Joint Channel Access and Sampling Rate Control in Energy Harvesting Cognitive Radio Sensor Networks

Ju Ren, *Student Member, IEEE,* Yaoxue Zhang, Ruilong Deng, *Member, IEEE,* Ning Zhang, *Member, IEEE,* Deyu Zhang, and Xuemin (Sherman) Shen *Fellow, IEEE*

Abstract—In this paper, we investigate the network utility maximization problem in energy harvesting cognitive radio sensor networks (CRSNs). Different from traditional sensor networks, sensor nodes in CRSNs are embedded cognitive radio modules, enabling them to dynamically access the licensed channels. Since the dynamic channel access is critical to guarantee the network capacity for CRSNs, existing solutions without considering the dynamic channel access cannot be directly applied into CRSNs. To this end, we aim at maximizing the network utility by jointly controlling the sampling rates and channel access of sensor nodes, under the energy consumption, channel capacity and interference constraints. With the consideration of fluctuated energy harvesting rates and channel switching costs, we formulate the network utility maximization as a mix-integer non-linear programming problem and solve it in an efficient and decoupled way by means of dual decomposition. A joint channel access and sampling rate control scheme, named JASC, is then proposed considering the real-time channel sensing results and energy harvesting rates. Extensive simulation results demonstrate that JASC can efficiently improve the network utility in CRSNs based on a realistic energy harvesting dataset.

Index Terms—cognitive radio sensor network, energy harvesting, sampling rate control, dynamic channel access, network utility maximization.

1 Introduction

As a promising data gathering technique, wireless sensor network (WSN) has been widely applied and becomes one of the significant and fundamental networks in the foreseeable era of Internet of things and big data [1], [2]. However, since sensor nodes are generally low-cost and battery-powered, the development and spread of WSN are limited by the highly-constrained network lifetime. The emergence and maturation of energy harvesting technology provides a solution to address this issue by enabling sensor nodes to harvest energy from the ambient environment [3], which greatly accelerates the flourish of WSN applications in recent years. On the other hand, as the explosion of wireless services makes the unlicensed spectrum increasingly crowded, WSNs operating over the unlicensed spectrum suffer from heavy interference caused by the applications using the same spectrum. Cognitive Radio (CR) technique has been developed as an efficient way to address the spectrum scarcity problem by enabling opportunistic access to the licensed spectrum bands [4]. This technology can also be applied to WSNs, giving rise to Cognitive Radio Sensor Networks (CRSNs).

In CRSNs, sensor nodes can opportunistically access licensed channels for data transmission and reception by adjusting their radio configuration, when the licensed channels are sensed as available. As a result, the dynamic channel access becomes critical to guarantee the quality-of-service (QoS) for CRSNs. In this regard, a number of existing works provide comprehensive investigation to reduce transmission delay [5]–[8] and improve network capacity [9], [10], laying a solid foundation for studying the dynamic channel access in CRSNs. Meanwhile, for most of data-gathering WSN applications, network utility is an important indicator to evaluate data collection efficiency. Since network utility depends on the sampling rates of sensor nodes and network capacity, it motivates us to jointly study the sampling rate control and dynamic channel access to optimize the network utility in CRSNs.

To this end, this paper focuses on the network utility maximization problem in energy harvesting CRSNs. Different from the existing works that maximize the network utility for the WSNs with a fixed and stable network capacity, the dynamic channel access leads to a dynamic network capacity in CRSNs. Therefore, network utility maximization in energy harvesting CRSNs faces a great challenge of scheduling channel access for sensor nodes, in addition to the inherent challenges such as sampling rate controlling and stochastic renewable energy constraints.

- *Ju Ren, Yaoxue Zhang and Deyu Zhang are with the College of Information Science and Engineering, Central South University, Changsha, Hunan Province, China, 410083. E-mail: {ren_ju, zyx, zdy876}@csu.edu.cn.*
- *Ruilong Deng is with the Department of Electrical and Computer Engineering, University of Alberta, , Edmonton, AB, Canada T6G 1H9. E-mail: ruilong@ualberta.ca.*
- *Ning Zhang and Xuemin (Sherman) Shen are with the Department of Electrical and Computer Engineering, University of Waterloo, Waterloo, ON, Canada, N2L 3G1. E-mail: {n35zhang, xshen}@bbcr.uwaterloo.ca. Dr. Ning Zhang is the corresponding author of this paper.*

This article has been accepted for publication in a future issue of this journal, but has not been fully edited. Content may change prior to final publication. Citation information: DOI 10.1109/TETC.2016.2555806, IEEE Transactions on Emerging Topics in Computing

In this paper, we investigate the network utility maximization problem in energy harvesting CRSNs by jointly considering the sampling rate control and channel access. The network operation is divided into different energy harvesting cycles, each of which is time slotted for dynamic channel access. Since the energy consumption for sensing the availability of licensed channels is considerable for sensor nodes, a spectrum market is introduced to take charge of channel sensing at each time slot and use the historical sensing results to predict the channel availability information for the CRSN. Sensor nodes are scheduled to access the available channels under the channel interference constraint at each time slot. The network utility is defined as increasing with the amount of sensory data collected by the CRSN and decreasing with the capacity of the accessed channels. Consequently, the network utility would be greatly impacted by sampling rate control and channel access schedule, under the harvested energy, channel capacity and interference constraints. Therefore, we jointly optimize the channel access and sampling rates and propose an efficient algorithm to maximize the network utility. Specifically, the contributions of this paper are three-fold.

(i) With the consideration of fluctuated energy harvesting rates and energy consumption in channel switching, we formulate the network utility maximization problem as a mixed-integer nonlinear optimization problem (MINLP), to determine the optimal channel access and sampling rate for each sensor node at different time slots.
(ii) To address the MINLP, we decouple the primal problem into two independent subproblems by dual decomposition and present two efficient solutions for the subproblems. Based on the subproblem solutions, a subgradient method based algorithm is proposed to solve the network utility maximization problem.
(iii) To mitigate the impact of prediction error, we further propose a Joint channel Access and Sampling rate Control scheme, named JASC, to maximize the network utility, which can determine the sampling rates and accessed channels of sensor nodes at each time slot, adapting to the real-time channel sensing results and energy harvesting rates.

The remainder of this paper is organized as follows. Section 2 reviews the related works. The system model and problem formulation are introduced in Section 3. In Section 4, we decouple the network utility maximization problem into two subproblems by dual decomposition. Section 5 presents the solutions of the two subproblems. The joint channel access and sampling rate control scheme is proposed in Section 6. Simulation results are provided in Section 7 to evaluate the performance of the proposed scheme. Finally, Section 8 concludes the paper and outlines our future work.

2 Related Works

Recently, the network utility maximization problem has attracted considerable attention in traditional energy harvesting WSNs. Liu *et al.* [11] propose a QuickFix algorithm to maximize the network utility by determining the sampling rates and routes for sensor nodes. To adjust the sampling rates adaptive to battery levels, a local algorithm, called SanpIt, is developed to sustain the network operation. Deng *et al.* [12] investigate the network utility maximization problem with spatiotemporally-coupled constraints in rechargeable sensor networks. To address the problem, they propose a distributed algorithm to jointly optimize the sampling rates and battery levels to achieve the globally optimal solution. Different from the aforementioned works maximizing the network utility based on predictable energy harvesting rates, Chen *et al.* [13] propose an online solution to address the energy allocation and routing problem for maximizing the network utility without prior knowledge of the replenishment profile. Huang and Neely [14] investigate the general network utility maximization problem in energy harvesting networks. They propose an online algorithm to jointly manage the harvested energy and adjust transmit power to optimize the time-average expected network utility and guarantee the network stability and energy supply. Besides the discussed works, Zhao *et al.* [13] develop a distributed algorithm to adjust the sampling rates of sensor nodes for maximizing network utility, by leveraging a mobile entity as mobile data collector and energy transporter. In [15] and [16] , limited battery capacity is considered and studied for the optimization of sampling rates in energy harvesting WSNs.

Most of existing solutions can effectively improve the network utility and manage the harvested energy in traditional energy harvesting WSNs [17]. However, since the dynamic channel access becomes a new challenge for maximizing the network utility in CRSNs, existing solutions cannot be directly applied into CRSNs. As an emerging solution to the spectrum scarcity problem, CRSN, especially the dynamic channel access in CRSN, has also been well studied to improve the network performances in recent literatures, in terms of delay, throughput and energy efficiency.

Liang *et al.* [5] analyze the delay performance of dynamic channel access to support real-time traffic in CRSNs. They derive the average packet transmission delay for two types of channel switching mechanisms, called periodic switching and triggered switching, under two kinds of real-time traffic, including periodic data traffic and Poisson traffic, respectively. Quang and Kim [9] develop a throughput-aware routing scheme to improve network throughput and decrease end-to-end delay for a large-scale clustered CRSN based on ISA100.11a. Han *et al.* [18] propose a channel management scheme for CRSNs, which can adaptively choose the operation mode of the network in terms of channel sensing, channel switching, and data trans-

This article has been accepted for publication in a future issue of this journal, but has not been fully edited. Content may change prior to final publication. Citation information: DOI 10.1109/TETC.2016.2555806, IEEE Transactions on Emerging Topics in Computing

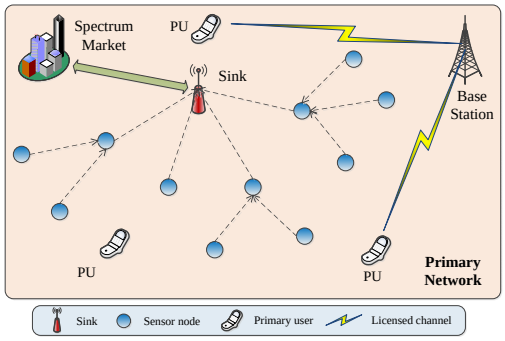

Fig. 1. The architecture of CRSN.

mission/reception, for energy efficiency improvement according to the outcome of channel sensing. In addition, opportunistic medium access (MAC) protocol design and performance analysis are studied to support the dynamic channel access for CRSNs in [19]–[21]. Motivated by the superior energy efficiency of clustering, dynamic spectrum-aware clustering strategies are also investigated in [22], [23] to improve energy efficiency and spectrum utilization for CRSNs.

However, to the best of our knowledge, the network utility maximization problem, with the consideration of energy management, dynamic channel access and interference control, has not been investigated in CRSNs.

3 System Model and Problem Formulation

3.1 Network Model

Consider a cognitive radio sensor network with a set of cognitive sensor nodes $\mathcal{N} = \{1, ..., N\}$ distributed to monitor an area of interest, as shown in Fig. 1. Each sensor node is equipped with energy harvesting devices to harvest energy from ambient environment and a rechargeable battery to store the harvested energy. The time cycle of the network is defined as an energy harvesting period $\mathcal{T}$, and each time cycle is divided into a set of time slots $\mathcal{T} = \{1, ..., T\}$. During each time slot t, sensor node i senses the monitored area with a sampling rate $s_{i,t}$ and transmits the sensory data to the sink via a static multi-hop routing path, which makes the network topology be a tree with the sink as the root.

The sensor nodes originally work on a unlicensed channel (e.g., 2.4 GHz), but they are embedded with cognitive radio modules, which enable them to opportunistically access licensed channels by adjusting their radio parameters. Meanwhile, there are a number of overlapping wireless applications working on the same unlicensed channel, causing significant and uncontrollable interference to the CRSN. As a result, sensor nodes have to sense and access licensed channels for data transmission to guarantee the required network performances (e.g., delay and throughput). There are a set of licensed channels $\mathcal{C} = \{1, ..., K\}$ with different channel capacities $\{C_1, ..., C_K\}$ in the primary network coexisting with the CRSN [1]. The primary user (PU) behavior is assumed to be stationary and ergodic over the K channels. The cognitive sensor nodes of the CRSN are secondary users (SUs) in the primary network and can opportunistically access the idle licensed channels. There exists a spectrum market that is in charge of channel sensing and providing available licensed channel information to SUs (e.g., sensor nodes in the CRSN). At the beginning of each time slot, the spectrum market senses the licensed channels and provide the available channels that can be accessed during the time slot. Denote the available licensed channel set at time slot t as $\mathcal{C}_t$, and we have $\mathcal{C}_t \subseteq \mathcal{C}$. Due to the stochastic PU traffic over the licensed channels, the available licensed channel set $\mathcal{C}_t$ may vary at different time slots. Moreover, at each time slot t, the spectrum market can predict the availability of each licensed channel $k \in \mathcal{C}$ for the next T time slots based on historical channel sensing results with high accuracy, by hidden Markov models [24] or neural networks [25]. In other words, the CRSN can obtain the predicted available channel sets $\{\mathcal{C}_1, ..., \mathcal{C}_T\}$ over the whole period $\mathcal{T}$.

During each time slot t, the CRSN schedules each node i to access a licensed channel $k \in \mathcal{C}_t$ to transmit its data. To coordinate the channel accessing, a common channel is assumed to be available to exchange control information among sensor nodes and the sink. To ease the presentation, the key notations are listed in Table 1.

3.2 Communication Link Model

According to the network model, node i senses data at $s_{i,t}$ and transmits its sensory data via a fixed routing path to the sink. Let $\mathcal{R}_i$ be the set of relays for node i, $\mathcal{A}_i \triangleq \{j \mid i \in \mathcal{R}_j\}$ be the set of ancestors that use node i as a relay along their routing paths, and $\mathcal{B}_i$ denote the set of brothers that have the same next hop as node i. There are only a transmitter and a receiver embedded in each sensor node as well as the sink. Both of transmitter and receiver can independently adjust their radio parameters to use a specific channel independently. It indicates that each sensor node should transmit or receive data over a single channel, but the channels used for data transmission and reception can be different.

We use a binary variable $z_{i,t,k}$ to denote whether node i's transmitter is scheduled to access channel k during time slot t. If i is scheduled to access channel k, $z_{i,t,k} = 1$; otherwise, $z_{i,t,k} = 0$. Since each transmitter can only access a specific channel, we have

$$\sum_{k \in \mathcal{C}_t} z_{i,t,k} = 1, \ \forall i \in \mathcal{N}, \forall t \in \mathcal{T}. \quad (1)$$

Meanwhile, each data receiver, including each relay node and the sink, can only receive data over a specific

1. TV white spaces are the considered licensed channels in our network scenario. A TV tower is the primary user in the primary network, which can make the availability of each licensed channel the same to all the sensor nodes.

This article has been accepted for publication in a future issue of this journal, but has not been fully edited. Content may change prior to final publication. Citation information: DOI 10.1109/TETC.2016.2555806, IEEE Transactions on Emerging Topics in Computing

TABLE 1
The Key Notations

Notation	Definition
$\mathcal{N}$,$\mathcal{T}$,$\mathcal{C}$	Set of sensor nodes, time slots and licensed channels
i or j	Index of sensor node
t or h, k	Index of time slot and licensed channel
$\mathcal{C}_t$	Available channel set at time slot t
$\mathcal{A}$, $\mathcal{R}$, $\mathcal{B}$	Set of ancestors, relays and neighbors
$s_{i,t}$, $\boldsymbol{S}$	i's sampling rate at time slot t, sampling rate matrix
$z_{i,t,k}$, $\boldsymbol{Z}$	0-1 variable denoting whether i accesses channel k at time slot t, channel access decision matrix
$D_{i,t}$	i's data transmission rate at time slot t
C_k	Capacity of channel k
e_s, e_t, e_r, e_w	Energy consumption for data sensing, transmitting, receiving and channel switching
$\phi_{i,t}$	Energy consumption rate of node i at time slot t
$E^w_{i,t}$	i's channel switching energy consumption at t
$R^u_{i,t}$	Energy consumption upper bound of i at time slot t
Δt	Duration of a time slot
$\mathcal{I}_i$, $\mathcal{S}_i$	Interference set of node i, set of node i's sons
$\psi_{i,t}$	i's energy harvesting rate at time slot t
$I(a)$	Indicator function, if a is true, $I(a)=1$; otherwise, $I(a)=0$
φ	Channel cost for the channel with unit capacity
$\boldsymbol{\alpha}$, $\boldsymbol{\beta}$	Lagrangian multiplier matrices
$\boldsymbol{\lambda}$, $\boldsymbol{\mu}$, $\boldsymbol{\eta}$	Intermediate variable matrices
$y_{i,t,k}$, $\boldsymbol{Y}$	0-1 variable denoting whether TRS p accesses channel k at time slot t, channel access decision matrix
$\mathcal{Q}_p$, $\mathcal{N}_p$	Set of transmitters in TRS p, Set of sensor nodes (including transmitters and the receiver) in TRS p

channel, which indicates that node i and its brothers should access the same channel. Thus, we have,

$$z_{i,t,k} = z_{j,t,k}, \quad \forall j \in \mathcal{B}_i, \forall k \in \mathcal{C}, \forall i \in \mathcal{N}, \forall t \in \mathcal{T}. \quad (2)$$

Furthermore, if node i and the nodes of $\mathcal{B}_i$ are scheduled to access channel k, the channel capacity should be no less than the sum of node i's transmission rate and its brothers' transmission rates to avoid link congestion. Let $D_{i,t}$ be the data transmission rate of node i, then we have $D_{i,t} = s_{i,t} + \sum_{j\in\mathcal{A}_{i,t}} s_{j,t}$, and the link capacity constraint

$$D_{i,t} + \sum_{j\in\mathcal{B}_{i,t}} D_{j,t} \le \sum_{k\in\mathcal{C}_t} z_{i,t,k} C_k, \ \forall i \in \mathcal{N}, \forall t \in \mathcal{T}. \quad (3)$$

Actually, the utilization of channel capacity C_k depends on the number of nodes in $\mathcal{B}_{i,t}$ and the adopted MAC protocol. To focus on the network utility optimization in high network layers, we consider that the MAC protocol can provide full utilization of the channel capacity.

3.3 Energy Harvesting and Consumption Model

Let $\psi_{i,t}$ denote the energy harvesting rate of node i at time slot t, which is assumed to be stable during the time slot and can be predicted with high accuracy for the next T time slots. Each sensor node consumes energy in data sensing, transmitting and receiving. For each node i, let e_s, e_t and e_r be the energy consumption rates for data sensing, transmitting and receiving, respectively. Thus, during each time slot t, the energy consumption rate $\phi_{i,t}$ of node i is defined as

$$\phi_{i,t} \triangleq (e_s + e_t) \cdot s_{i,t} + (e_r + e_t) \cdot \sum_{j\in\mathcal{A}_i} s_{j,t}. \quad (4)$$

In addition, there is energy consumption associated with node i for channel switching, if its accessed channel changes from time slot $t-1$ to t. Let $\mathcal{S}_i$ be the set of i's sons who use i as the next hop, and s be one of the sensor nodes in $\mathcal{S}_i$. Therefore, for each $i \in \mathcal{N}$, i's energy consumption for channel switching is $E^w_{i,t} \triangleq \sum_{k\in\mathcal{C}_t} I(z_{s,t-1,k} \neq z_{s,t,k}) e_w z_{i,t,k} + \sum_{k\in\mathcal{C}_t} I(z_{i,t-1,k} \neq z_{i,t,k}) e_w z_{i,t,k}$, where e_w is the energy consumption for channel switching, and $I(a)$ is an indicator function such that if a is true, $I(a)=1$; otherwise, $I(a)=0$. Note that, if node i is a leaf node, $\mathcal{S}_i = \emptyset$ and $I(z_{s,t-1,k} \neq z_{s,t,k}) = 0$.

We assume that the battery capacity is large enough to store the harvested energy, such that we only focus on controlling the energy consumption rates to guarantee the sustainability of sensor nodes. Let Δt be the duration of each time slot and $r_{i,t}$ be i's residual energy at the end of time slot t. Then, we have $r_{i,t} = r_{i,t-1} + \psi_{i,t}\Delta t - \phi_{i,t}\Delta t - E^w_{i,t}$. Denote $r_{i,0}$ as i's initial energy, which is known in advance. $r_{i,t}$ can be recursively calculated as

$$r_{i,t} = r_{i,0} + \sum_{h=1}^{t} \psi_{i,h}\Delta t - \sum_{h=1}^{t} \phi_{i,h}\Delta t - \sum_{h=1}^{t} E^w_{i,h}. \quad (5)$$

In order to guarantee that sensor nodes have enough energy to switch channel at the beginning of each time slot t, we have $r_{i,t} \ge r_{i,w}$, where $r_{i,w}$ is i's reserved energy for channel switching. If i is a leaf node, $r_{i,w} = e_w$; otherwise $r_{i,w} = 2e_w$. Therefore, for each node i at time slot t, we have the following energy consumption constraint:

$$r_{i,0} + \sum_{h=1}^{t} \psi_{i,h}\Delta t - \sum_{h=1}^{t} \phi_{i,h}\Delta t - \sum_{h=1}^{t} E^w_{i,h} \ge r_{i,w}. \quad (6)$$

Since $r_{i,0}$, $r_{i,w}$ and $\sum_{h=1}^{t} \psi_{i,h}\Delta t$ are constant in the constraint, we define the energy consumption upper bound as $R^u_{i,t} \triangleq r_{i,0} + \sum_{h=1}^{t} \psi_{i,h}\Delta t - r_{i,w}$ and rewrite the energy consumption as

$$\sum_{h=1}^{t} \phi_{i,h}\Delta t + \sum_{h=1}^{t} E^w_{i,h} \le R^u_{i,t}, \ \forall i \in \mathcal{N}, \forall t \in \mathcal{T}. \quad (7)$$

3.4 Channel Interference Model

Due to the broadcast nature of wireless channels, sensor nodes may cause interference to the sensor nodes within their interference range, if they are scheduled to access the same channel [26]. Since all the sensor nodes have a fixed transmission power, the interference range of each sensor node is also fixed. For two communication links $a \to b$ and $c \to d$, if node d (or b) is in the interference range of node a (or c), a and c cannot operate on the same

This article has been accepted for publication in a future issue of this journal, but has not been fully edited. Content may change prior to final publication. Citation information: DOI 10.1109/TETC.2016.2555806, IEEE Transactions on Emerging Topics in Computing

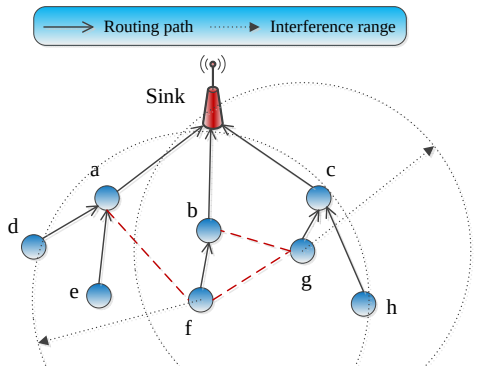

Fig. 2. Interference set illustration.

channel to avoid interference. Let $\mathcal{I}_i$ be the interference set of node i, which consists of the sensor nodes that cannot access the same channel as node i. Therefore, for $\forall i \in \mathcal{N}$, we have

$$\sum_{k\in\mathcal{C}_t} (z_{i,t,k} \cdot z_{j,t,k}) = 0, \quad \forall j \in \mathcal{I}_i, \forall t \in \mathcal{T}, \tag{8}$$

where the interference set $\mathcal{I}_i$ has no intersection with $\mathcal{B}_i$, i.e., $\mathcal{I}_i \cap \mathcal{B}_i = \emptyset$. Fig. 2 illustrates a specific case with channel interference. According to the interference definition, we have $\mathcal{I}_a = \{f\}$, $\mathcal{I}_b = \{e, g, h\}$, $\mathcal{I}_c = \{f\}$, $\mathcal{I}_d = \{f\}$, $\mathcal{I}_e = \{f\}$, $\mathcal{I}_f = \{a, c, d, e, g, h\}$, $\mathcal{I}_g = \{b, f\}$ and $\mathcal{I}_h = \{f\}$.

3.5 Problem Formulation

The objective is to maximize the network utility by controlling the sampling rate $s_{i,t}$ and determining the channel access $z_{i,t,k}$ for each node i over a period $\mathcal{T}$. The network utility is defined as the utility of sensory data subtracting the channel cost [11], [12], while the sensory data utility and channel cost are specifically defined as follows. Let $V(i,t)$ be the utility of i's sensory data at time slot t. Then, the total utility of sensory data is $V \triangleq \sum_{t\in\mathcal{T}} \sum_{i\in\mathcal{N}} V(i,t)$. The utility function $V(\cdot)$ is assumed to be increasing and strictly concave to guarantee the fairness for sensor nodes [12]. For example, $V(i,t) = \log(1 + s_{i,t})$. On the other hand, since the spectrum market periodically senses the licensed channels and provides the available channel information to the CRSN, the CRSN should pay for the channels accessed by sensor nodes, which is defined as channel cost. We consider that the channel cost depends on the total channel capacity of the accessed channels. Let φ be the cost for the channel with unit capacity, then, the channel cost is $W \triangleq \sum_{t\in\mathcal{T}} \sum_{k\in\mathcal{C}_t} \left(I(\sum_{i\in\mathcal{N}} z_{i,t,k} \neq 0) \cdot \varphi C_k\right)$, where $I(\sum_{i\in\mathcal{N}} z_{i,t,k} \neq 0)$ is to indicate whether channel k is accessed by the CRSN. In summary, the network utility is defined as

$$U \triangleq \sum_{t\in\mathcal{T}} \sum_{i\in\mathcal{N}} \log(1 + s_{i,t}) - \sum_{t\in\mathcal{T}} \sum_{k\in\mathcal{C}_t} \left(I\left(\sum_{i\in\mathcal{N}} z_{i,t,k} \neq 0\right) \varphi C_k \right). \tag{9}$$

Let a matrix $\boldsymbol{S} \triangleq \{s_{i,t} \mid \forall i \in \mathcal{N}, \forall t \in \mathcal{T}\}$ and a binary matrix $\boldsymbol{Z} = \{z_{i,t,k} \mid \forall i \in \mathcal{N}, \forall t \in \mathcal{T}, \forall k \in \mathcal{C}_t\}$ denote the allocated sampling rates and channels for sensor nodes over time period $\mathcal{T}$, respectively, the network utility maximization problem can be formulated as

$$\textbf{(NUMP)} \quad \max_{\boldsymbol{S},\boldsymbol{Z}} \; U$$
$$\text{s.t.} \begin{cases} (1),\ (2),\ (3),\ (7) \text{ and } (8) \\ s_{i,t} \geq 0 \\ z_{i,t,k} = 0 \text{ or } 1, \forall k \in \mathcal{C}_t \end{cases}, \ \forall i \in \mathcal{N}, \forall t \in \mathcal{T}.$$

Since Eq. (8) is a non-linear constraint, **(NUMP)** is a mix-integer non-linear optimization problem, which is challenging to solve. In the following section, we will focus on solving this intractable optimization problem.

4 Problem Decomposition and Solution

In this section, we aim to decouple **(NUMP)** into separable subproblems by dual decomposition, and then tackle the subproblems separately and efficiently.

4.1 Lagrangian

Since Eq. (3) and (7) are the constraints coupling the two decision variable matrices $\boldsymbol{S}$ and $\boldsymbol{Z}$, we can decouple them by relaxing these two constraints with Lagrangian relaxation. We introduce two Lagrangian multiplier matrices $\boldsymbol{\alpha} \triangleq \{\alpha_{i,t} \mid \forall i \in \mathcal{N}, \forall t \in \mathcal{T}\}$ and $\boldsymbol{\beta} \triangleq \{\beta_{i,t} \mid \forall i \in \mathcal{N}, \forall t \in \mathcal{T}\}$, and define the Lagrangian associated with the primal problem **(NUMP)** as

$$\begin{aligned} \mathcal{L}(\boldsymbol{\alpha}, \boldsymbol{\beta}) = & \sum_{t\in\mathcal{T}} \sum_{i\in\mathcal{N}} \log(1 + s_{i,t}) \\ & - \sum_{t\in\mathcal{T}} \sum_{k\in\mathcal{C}_t} \left(I\left(\sum_{i\in\mathcal{N}} z_{i,t,k} \neq 0\right) \varphi C_k \right) \\ & + \sum_{t\in\mathcal{T}} \sum_{i\in\mathcal{N}} \alpha_{i,t} \left[\sum_{k\in\mathcal{C}_t} z_{i,t,k} C_k - D_{i,t} - \sum_{j\in\mathcal{B}_{i,t}} D_{j,t} \right] \\ & + \sum_{t\in\mathcal{T}} \sum_{i\in\mathcal{N}} \beta_{i,t} \left[R^u_{i,t} - \sum_{h=1}^{t} \phi_{i,h} \Delta t - \sum_{h=1}^{t} E^w_{i,h} \right], \end{aligned} \tag{10}$$

where the Lagrangian multipliers $\alpha_{i,t}$ and $\beta_{i,t}$ should be no less than 0, i.e., $\alpha_{i,t} \geq 0$ and $\beta_{i,t} \geq 0$, $\forall i \in \mathcal{N}, \forall t \in \mathcal{T}$. According to the communication link model, we have

$$\begin{cases} \sum_{i\in\mathcal{N}} \alpha_{i,t} \left(D_{i,t} + \sum_{j\in\mathcal{B}_i} D_{j,t} \right) = \sum_{i\in\mathcal{N}} D_{i,t} \left(\alpha_{i,t} + \sum_{j\in\mathcal{B}_i} \alpha_{j,t} \right) \\ \sum_{i\in\mathcal{N}} \alpha_{i,t} \left(s_{i,t} + \sum_{j\in\mathcal{A}_i} s_{j,t} \right) = \sum_{i\in\mathcal{N}} s_{i,t} \left(\alpha_{i,t} + \sum_{j\in\mathcal{R}_i} \alpha_{j,t} \right) \end{cases} \tag{11}$$

This article has been accepted for publication in a future issue of this journal, but has not been fully edited. Content may change prior to final publication. Citation information: DOI 10.1109/TETC.2016.2555806, IEEE Transactions on Emerging Topics in Computing

Thus, if we define the following intermediate variables

$$\begin{cases} \lambda_{i,t} \triangleq \alpha_{i,t} + \sum\limits_{j\in\mathcal{B}_i} \alpha_{j,t} + \sum\limits_{j\in\mathcal{R}_i} \left[\alpha_{j,t} + \sum\limits_{x\in\mathcal{B}_j} \alpha_{x,t}\right] \\ \mu_{i,t} \triangleq \sum\limits_{h=1}^{t} \left[\beta_{i,h}(e_s+e_t) + \sum\limits_{j\in\mathcal{R}_i} \beta_{j,h}(e_r+e_t)\right]\cdot\Delta t \\ \eta_{i,t} \triangleq \sum\limits_{h=1}^{t} \beta_{i,h} \end{cases}, \tag{12}$$

the Lagrangian can be rewritten as

$$\begin{aligned} \mathcal{L}(\boldsymbol{\alpha},\boldsymbol{\beta},\boldsymbol{S},\boldsymbol{Z}) &= \sum_{t\in\mathcal{T}}\sum_{i\in\mathcal{N}} \Big[\log(1+s_{i,t}) - (\lambda_{i,t}+\mu_{i,t})s_{i,t}\Big] \\ &- \sum_{t\in\mathcal{T}}\sum_{k\in\mathcal{C}_t} \left(I\left(\sum_{i\in\mathcal{N}} z_{i,t,k}\neq 0\right)\cdot\varphi C_k\right) \\ &+ \sum_{t\in\mathcal{T}}\sum_{i\in\mathcal{N}} \left[\alpha_{i,t}\sum_{k\in\mathcal{C}_t} z_{i,t,k}C_k - \eta_{i,t}E^w_{i,t} + \beta_{i,t}R^u_{i,t}\right]. \end{aligned} \tag{13}$$

4.2 Problem Decomposition and Dual Problem

Based on the Lagrangian (13), the dual function (i.e., the objective function of the dual problem) is the maximum value of the Lagrangian over $\boldsymbol{S}$ and $\boldsymbol{Z}$:

$$\mathcal{D}(\boldsymbol{\alpha},\boldsymbol{\beta}) = \sup_{\boldsymbol{S},\boldsymbol{Z}} \mathcal{L}(\boldsymbol{\alpha},\boldsymbol{\beta},\boldsymbol{S},\boldsymbol{Z}). \tag{14}$$

Due to the separability of the two variable matrices, we define two subproblems to decouple $\boldsymbol{S}$ and $\boldsymbol{Z}$:

$$\textbf{(SP1)}\ D_1(\boldsymbol{\alpha},\boldsymbol{\beta}) \triangleq \max_{\boldsymbol{S}} \sum_{t\in\mathcal{T}}\sum_{i\in\mathcal{N}} \Big[\log(1+s_{i,t}) - (\lambda_{i,t}+\mu_{i,t})s_{i,t}\Big]$$
$$\text{s.t. } s_{i,t}\geq 0,\ \forall i\in\mathcal{N},\forall t\in\mathcal{T}.$$

$$\textbf{(SP2)}\ D_2(\boldsymbol{\alpha},\boldsymbol{\beta}) \triangleq \max_{\boldsymbol{Z}} \sum_{t\in\mathcal{T}}\sum_{i\in\mathcal{N}} \left[\alpha_{i,t}\sum_{k\in\mathcal{C}_t} z_{i,t,k}C_k - \eta_{i,t}E^w_{i,t}\right] - \sum_{t\in\mathcal{T}}\sum_{k\in\mathcal{C}_t} \left(I\left(\sum_{i\in\mathcal{N}} z_{i,t,k}\neq 0\right)\cdot\varphi C_k\right)$$
$$\text{s.t. } \begin{cases}(1),\ (2) \text{ and } (8)\\ z_{i,t,k}=0 \text{ or } 1,\ \forall k\in\mathcal{C}_t\end{cases},\ \forall i\in\mathcal{N},\forall t\in\mathcal{T}.$$

Based on the definition of **(SP1)** and **(SP2)**, the dual function can be rewritten as

$$\mathcal{D}(\boldsymbol{\alpha},\boldsymbol{\beta}) = D_1(\boldsymbol{\alpha},\boldsymbol{\beta}) + D_2(\boldsymbol{\alpha},\boldsymbol{\beta}) + \sum_{t\in\mathcal{T}}\sum_{i\in\mathcal{N}} \beta_{i,t}R^u_{i,t}. \tag{15}$$

The dual problem is to minimize the dual function over the Lagrangian multiplier matrices $\boldsymbol{\alpha}$ and $\boldsymbol{\beta}$:

$$\textbf{(DP-NUMP)}\ \min_{\boldsymbol{\alpha},\boldsymbol{\beta}} \mathcal{D}(\boldsymbol{\alpha},\boldsymbol{\beta})$$
$$\text{s.t. } \alpha_{i,t},\beta_{i,t}\geq 0,\ \forall i\in\mathcal{N},\forall t\in\mathcal{T}.$$

According to the analysis and proof in [27], [28], only weak duality can be guaranteed by Lagrangian relaxation, which indicates that there exists a duality gap between the optimal solutions to the dual problem and the primal problem. Let O_p and O_d be the optimal results of **(NUMP)** and **(DP-NUMP)**. We have, $O_p \leq O_d$ holds for all feasible solutions and O_d actually becomes the upper bound of O_p [29].

4.3 Subgradient Method for Solving Dual Problem

Given $\boldsymbol{\alpha}$ and $\boldsymbol{\beta}$, if we can address **(SP1)** and **(SP2)** separately, the dual problem **(DP-NUMP)** can be iteratively solved using a subgradient method. Specifically, during each iteration, the Lagrangian multipliers are updated in an opposite direction to the partial gradient of the Lagrangian dual function [12], [30], i.e.,

$$\begin{cases} \alpha_{i,t}(m+1) = [\alpha_{i,t}(m) - \gamma_\alpha\cdot f_{\alpha,i,t}(m)]^+ \\ \beta_{i,t}(m+1) = [\beta_{i,t}(m) - \gamma_\beta\cdot f_{\beta,i,t}(m)]^+ \end{cases} \tag{16}$$

where $m\in\mathbb{N}^+$ is the iteration index; $\gamma_\alpha>0$ and $\gamma_\beta>0$ are the step sizes adjusting the convergence rate; $[a]^+ \triangleq \max\{a,0\}$ and $f_{\alpha,i}(m)$ and $f_{\beta,i}(m)$ are subgradients of dual function with respect to $\alpha_{i,t}$ and $\beta_{i,t}$, respectively,

$$\begin{cases} f_{\alpha,i,t}(m) = \dfrac{\partial\mathcal{D}(\boldsymbol{\alpha},\boldsymbol{\beta})}{\partial\alpha_{i,t}} = C_k - D_{i,t}(m) - \sum\limits_{j\in\mathcal{B}_i} D_{j,t}(m) \\ f_{\beta,i,t}(m) = \dfrac{\partial\mathcal{D}(\boldsymbol{\alpha},\boldsymbol{\beta})}{\partial\beta_{i,t}} = R^u_{i,t} - \sum\limits_{h=1}^{t}\phi_{i,h}(m)\Delta t - \sum\limits_{h=1}^{t} E^w_{i,h}(m). \end{cases} \tag{17}$$

Note that, $D_{i,t}(m)$ and $\sum_{h=1}^{t}\phi_{i,h}(m)$ can be calculated with $s_{i,t}(m)$, and $\sum_{h=1}^{t}E^w_{i,h}(m)$ can be calculated with $z_{i,t,k}$, while $s_{i,t}(m)$ and $z_{i,t,k}(m)$ can be obtained by solving **(SP1)** and **(SP2)** with given $\boldsymbol{\alpha}(m)$ and $\boldsymbol{\beta}(m)$. With sufficient iterations, the duality gap between the optimal values of $\mathcal{D}(\boldsymbol{\alpha},\boldsymbol{\beta})$ and U can be reduced to an acceptable threshold. The detailed algorithm for solving **(DP-NUMP)** and **(NUMP)** will be discussed in Section 6.1.

5 Subproblem Solutions

In this section, we solve the subproblems of the dual problem **(DP-NUMP)**. Due to the iteration process in addressing the dual problem, subproblems should be solved efficiently to guarantee the efficiency of our solution.

5.1 Optimal Solution for (SP1)

Given $\boldsymbol{\alpha}$ and $\boldsymbol{\beta}$, **(SP1)** becomes a separate optimization problem to maximize $D_1(\boldsymbol{\alpha},\boldsymbol{\beta})$ by determining the optimal sampling rates for sensor nodes at different time slots. Obviously, **(SP1)** is a convex optimization problem, due to the property of maximizing the concave objective function over a convex feasible set. **Proposition 1** provides the optimal solution of **(SP1)**.

Proposition 1. *If the optimal solution to* ***(SP1)*** *exists, i.e., the feasible set of* ***(SP1)*** *is not empty, the optimal sampling rate* $\boldsymbol{S^*}$ *is, for each* $i\in\mathcal{N}$ *and* $t\in\mathcal{T}$,

$$s^*_{i,t} = \frac{1}{\ln 2\cdot(\lambda_{i,t}+\mu_{i,t})} - 1. \tag{18}$$

Proof: Due to the convexity of **(SP1)**, the locally optimal solution is the globally optimal solution. Let $f(s_{i,t}) \triangleq \log(1+s_{i,t}) - (\lambda_{i,t}+\mu_{i,t})s_{i,t}$. Its first-order partial derivate is

$$\frac{\partial f}{\partial s_{i,t}} = \frac{1}{\ln 2\cdot(1+s_{i,t})} - \lambda_{i,t} - \mu_{i,t}. \tag{19}$$

This article has been accepted for publication in a future issue of this journal, but has not been fully edited. Content may change prior to final publication. Citation information: DOI 10.1109/TETC.2016.2555806, IEEE Transactions on Emerging Topics in Computing

By setting $\frac{\partial f}{\partial s_{i,t}} = 0$, we have $s_{i,t} = \frac{1}{\ln 2 \cdot (\lambda_{i,t} + \mu_{i,t})} - 1$. We set $s_{i,t}|_{\frac{\partial f}{\partial s_{i,t}}=0} \triangleq \frac{1}{\ln 2 \cdot (\lambda_{i,t} + \mu_{i,t})}$. Since $\frac{\partial f}{\partial s_{i,t}}$ is a monotonously increasing function over the constraint set of $s_{i,t}$, $f(s_{i,t})$ increases when $s_{i,t} \geq s_{i,t}|_{\frac{\partial f}{\partial s_{i,t}}=0}$ and the situation reverses when $s_{i,x} \leq s_{i,t}|_{\frac{\partial f}{\partial s_{i,t}}=0}$. Therefore, $f(s_{i,t})$ would achieve the maximum value at $s_{i,t}|_{\frac{\partial f}{\partial s_{i,t}}=0}$.

Meanwhile, since for each $i \in \mathcal{N}$ and $t \in \mathcal{T}$, $\alpha_{i,t} \geq 0$ and $\beta_{i,t} \geq 0$, we have $\lambda_{i,t} \geq 0$ and $\mu_{i,t} \geq 0$ according to Eq. (12). Thus, $s_{i,t}|_{\frac{\partial f}{\partial s_{i,t}}=0} > 0$. Since the feasible set of $f(s_{i,t})$ is $s_{i,t} \geq 0$, the optimal solution of $f(s_{i,t})$ is achieved at $s_{i,t}|_{\frac{\partial f}{\partial s_{i,t}}=0}$, i.e., $s^*_{i,t} = s_{i,t}|_{\frac{\partial f}{\partial s_{i,t}}=0} = \frac{1}{\ln 2 \cdot (\lambda_{i,t} + \mu_{i,t})} - 1$. □

5.2 Computational Complexity Analysis on (SP2)

Given $\boldsymbol{\alpha}$ and $\boldsymbol{\beta}$, **(SP2)** is a channel access problem to maximize $D_2(\boldsymbol{\alpha}, \boldsymbol{\beta})$ by determining the optimal binary matrix $\boldsymbol{Z}^*$. In the following, we prove that **(SP2)** is a NP-hard problem which cannot be optimally solved in polynomial time. We aim to reduce **(SP2)** to the vertex K-coloring problem (VKCP), which is a classic NP-hard problem. Before that, we first define VKCP as follows.

Definition 1. *The vertex K-coloring problem (VKCP): Given an undirected graph $\mathbb{G} = \{\mathbb{V}, \mathbb{E}\}$ and K colors, where K is an integer with $K \geq 0$, using at most K colors to find a coloring solution (i.e., assigning one of the K colors to each vertex) such that no two vertices sharing the same edge have the same color and the number of colors used to color the vertices is the smallest.*

Lemma 1. *VKCP is a NP-hard problem when $K \geq 3$.*

Proof: See Appendix A on the appendix file. □

The proof of **Lemma 1** can be found in [31] and [32]. In order to reduce **(SP2)** into VKCP, we reconstruct the problem as follows. We divide the network routing tree into a number of transmitter-receiver sets (TRSs). Each TRS consists of a data receiver and its sons. For a specific network routing tree, data receivers include all non-leaf sensor nodes and the sink. To illustrate the definition of TRS, Fig. 3 shows an example of dividing the network case in Fig. 2 into 4 TRSs. The red dash link between two TRSs denotes that there exists interference between them, which means any pair of connected TRSs cannot access the same channel to avoid interference.

According to the communication link model, the channel access in the CRSN is a receiver-based access problem, which means that the sensor nodes of each TRS should access the same channel for data transmission and reception. Let $\mathcal{P}$ denote the set of TRSs in the network. Then, the channel access problem changes to schedule each TRS $p \in \mathcal{P}$ to access a specific channel $k \in \mathcal{C}_t$. We use a binary matrix $\boldsymbol{Y} = \{y_{p,t,k} \mid \forall p \in \mathcal{P}, \forall t \in \mathcal{T}, \forall k \in \mathcal{C}_t\}$ to denote whether TRS p accesses channel k at time slot t. Meanwhile, if we let $\mathcal{Q}_p$ be the set of transmitters in TRS p, respectively, we have $z_{i,t,k} = y_{p,t,k} \mid \forall p \in \mathcal{P}, \forall t \in \mathcal{T}, \forall k \in \mathcal{C}_t$ for each $i \in \mathcal{Q}_p$. Then, the constraints of **(SP2)** can be rewritten as follows:

(a) Eq. (1) changes to $\sum_{k \in \mathcal{C}_t} y_{p,t,k} = 1, \ \forall \ p \in \mathcal{P}, t \in \mathcal{T}$;

(b) Eq. (2) is removed, since all the sensor nodes of a TRS can only access one channel;

(c) Eq. (8) changes to $\sum_{k \in \mathcal{C}_t} (y_{p,t,k} \cdot y_{q,t,k}) = 0, \ \forall q \in \mathcal{I}_p, \forall \ p \in \mathcal{P}, \forall t \in \mathcal{T}$, where $\mathcal{I}_p$ denotes the set of TRSs that may have interference with TRS p.

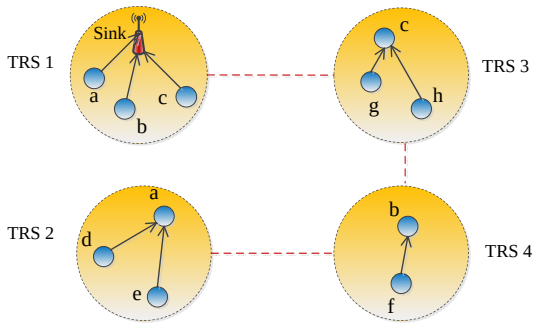

Fig. 3. Illustration of TRS definition.

Meanwhile, the objective function $D_2(\boldsymbol{\alpha}, \boldsymbol{\beta})$ can be rewritten with respect to $\boldsymbol{Y}$ as

$$TD_2(\boldsymbol{\alpha}, \boldsymbol{\beta}) = \sum_{t \in \mathcal{T}} \sum_{p \in \mathcal{P}} \left(\sum_{i \in \mathcal{Q}_p} \alpha_{i,t} \sum_{k \in \mathcal{C}_t} y_{p,t,k} C_k - \sum_{i \in \mathcal{N}_p} \beta_{i,t} E^w_{p,t} \right) - \sum_{t \in \mathcal{T}} \sum_{k \in \mathcal{C}_t} \left(I \left(\sum_{p \in \mathcal{P}} y_{p,t,k} \neq 0 \right) \cdot \varphi C_k \right), \tag{20}$$

where $\mathcal{N}_p$ denotes the set of sensor nodes in TRS p including the transmitters and receivers and $E^w_{p,t} \triangleq \sum_{k \in \mathcal{C}_t} I(y_{p,t-1,k} \neq y_{p,t,k}) e_w y_{p,t,k}$.

Thus, **(SP2)** can be transformed to an equivalent problem **(SP2-E)**, which is to determine $\boldsymbol{Y}$ to

$$\textbf{(SP2-E)} \quad \max_{\boldsymbol{Y_t}} TD_2(\boldsymbol{\alpha}, \boldsymbol{\beta})$$

$$\text{s.t.} \begin{cases} \sum_{k \in \mathcal{C}_t} y_{p,t,k} = 1 \\ \sum_{k \in \mathcal{C}_t} (y_{p,t,k} \cdot y_{q,t,k}) = 0, \ \forall q \in \mathcal{I}_p \\ y_{p,t,k} = 0 \text{ or } 1, \ \forall k \in \mathcal{C}_t \end{cases}, \forall p \in \mathcal{P}, \forall t \in \mathcal{T}.$$

Theorem 1. *In period $\mathcal{T}$, if there exists a time slot t with $|C_t| \geq 3$, **(SP2-E)** is NP-hard.*

Proof: See Appendix B on the appendix file. □

Corollary 1. *In period $\mathcal{T}$, if there exists a time slot t with $|C_t| \geq 3$, **(SP2)** is NP-hard.*

Corollary 1 always holds, since **(SP2)** is equivalent to **(SP2-E)**. We consider that the number of available channels provided by the spectrum market is usually larger than 3 [5], which means that we cannot obtain the optimal solution of **(SP2)** in polynomial time.

5.3 Suboptimal Solution for (SP2)

In the following, we propose a cross-entropy based heuristic algorithm (CEHA) to determine a suboptimal

This article has been accepted for publication in a future issue of this journal, but has not been fully edited. Content may change prior to final publication. Citation information: DOI 10.1109/TETC.2016.2555806, IEEE Transactions on Emerging Topics in Computing

solution for the problem in an efficient way. Due to the equivalence of **(SP2)** and **(SP2-E)**, we focus on solving **(SP2-E)** and use the solution of **(SP2-E)** to derive the solution of **(SP2)**. The main idea of cross-entropy methods is to transform a deterministic problem to an associated stochastic problem, which has been widely used in combinational optimization for suboptimal results [33].

CEHA defines a matrix $\boldsymbol{H} \triangleq \{H_{p,t,k} \mid \forall p \in \mathcal{P}, \forall t \in \mathcal{T}, \forall k \in \mathcal{C}_t\}$, where $H_{p,t,k}$ denotes the probability of TRS p accessing channel k at time slot t. For each $p \in \mathcal{P}$ at each $t \in \mathcal{T}$, $H_{p,t,k}$ is initialized as a specific value for each $k \in \mathcal{C}_t$ to make $\sum_{k \in \mathcal{C}_t} H_{p,t,k} = 1$. As a result, $\boldsymbol{H}_{p,t}(k) \triangleq Pr(X = k) = H_{p,t,k}$ is actually a PMF function for $k \in \mathcal{C}_t$. Then, CEHA finds the solution by an iterative procedure, where each iteration consists of two phases. In the first phase, a set of random samples are generated according to the PMF for each $p \in \mathcal{P}$ and $t \in \mathcal{T}$, which are used to calculate the corresponding solutions. In the second phase, the PMFs are updated based on some better solutions for the next iteration. Specifically, we describe the detailed procedures of CEHA as follows.

(1) *Constraint Relaxation* — We introduce a constant κ to relax the second constraint of **(SP2-E)**, which leads to the modified objective function

$$\overline{TD}_2(\boldsymbol{\alpha}, \boldsymbol{\beta}) = TD_2(\boldsymbol{\alpha}, \boldsymbol{\beta}) - \kappa \cdot \sum_{t \in \mathcal{T}} \sum_{p \in \mathcal{P}} \sum_{q \in \mathcal{I}_p} I\left(\sum_{k \in \mathcal{C}_t} (y_{q,t,k} \cdot y_{q,t,k}) \neq 0 \right)$$

where $\kappa \triangleq \sum_{t \in \mathcal{T}} \sum_{p \in \mathcal{P}} \sum_{i \in \mathcal{Q}_p} \sum_{k \in \mathcal{C}_t} \alpha_{i,t} C_k$ is a penalty to objective function if the constraint of $TD_2(\boldsymbol{\alpha}, \boldsymbol{\beta})$ is violated. Notably, κ is an upper bound of $TD_2(\boldsymbol{\alpha}, \boldsymbol{\beta})$ to guarantee that every feasible solution without violating the constraint will achieve a lower objective value than the infeasible solutions.

(2) *Initialization* — Initialize the maximum iteration number Γ and a difference threshold ϵ. Set the iteration counter $\tau = 1$. For each time slot t, we index the available channel set $\mathcal{C}_t$ as $\{1, ..., |\mathcal{C}_t|\}$, and set TRS p accesses each channel $k \in \mathcal{C}_t$ with equal probabilities, i.e., for each $k \in \mathcal{C}_t$, the PMF $\boldsymbol{H}^{\tau}_{p,t}$ is initialized as $\boldsymbol{H}^{\tau}_{p,t}(k) = H^{\tau}_{p,t,k} = \frac{1}{|\mathcal{C}_t|}$.

(3) *Sample Generation* —Use $\boldsymbol{H}^{\tau}_{p,t}$ to generate M values for each p and t. Each value denotes that p will access which channel at time slot t. For the m-th value X_m ($1 \leq m \leq M$), we create a binary string $x_{p,t,m}$ containing $|\mathcal{C}_t|$ digits, where the X_m-th digit is 1 and the other digits are 0. For example, if $|\mathcal{C}_t| = 4$ and $X_1 = 2$, we have $x_{p,t,1} = 0100$ which means p will access the 2nd channel in $\mathcal{C}_t$ at time slot t. Such that, M samples can be generated by the strings, with the m-th sample as $\{x_{p,t,m} \mid p \in \mathcal{P}, t \in \mathcal{T}\}$.

(4) *Sample Evaluation* — We use the M samples to calculate the corresponding values of $\overline{TD}_2(\boldsymbol{\alpha}, \boldsymbol{\beta})$. Note that, for the m-th sample, if the k-th digit of $x_{p,t,m}$ is 1, it denotes $y_{p,t,k} = 1$, and $y_{p,t,l} = 0$ for each $l \in \mathcal{C}_t - \{k\}$. Let θ_m be the value of $\overline{TD}_2(\boldsymbol{\alpha}, \boldsymbol{\beta})$ using the m-th sample. Then, sort the M values of $\overline{TD}_2(\boldsymbol{\alpha}, \boldsymbol{\beta})$ in a non-decreasing order and let Θ be the sorted set of the M values. We denote the corresponding samples of the first $\lceil \rho M \rceil$ values in Θ as a set $\mathcal{M}_{\rho}(\tau)$, which are called as "better" samples in this iteration.

(5) *PMF Update* — The PMF is updated based on $\mathcal{M}_{\rho}(\tau)$ in the iteration. For each $p \in \mathcal{P}$ and $t \in \mathcal{T}$, we update $\boldsymbol{H}^{\tau+1}$ as

$$H^{\tau+1}_{p,t,k} = \frac{\sum_{m \in \mathcal{M}_{\rho}(\tau)} G(x_{p,t,m}, k)}{\lceil \rho M \rceil}, \ k = 1, ..., |\mathcal{C}_t|,$$

where $G(a, b)$ is a function to obtain the k-th digit of a, e.g., $G(0100, 2) = 1$ and $G(0010, 2) = 0$.

(6) *Stopping Rule* — The iteration stops if either of the following two conditions is met. The first is the iteration count achieves the maximum iteration number Γ. The second is the difference of $\boldsymbol{H}^{\tau}$ and $\boldsymbol{H}^{\tau+1}$ is lower than a required threshold, i.e., $||\boldsymbol{H}^{\tau+1} - \boldsymbol{H}^{\tau}||_F \leq \epsilon$, where $||\cdot||_F$ is the Frobenius norm, and ϵ is the required threshold. Otherwise, set $\tau = \tau + 1$ and go back to step (2).

(7) *Result Output* — Generate a sample $\{x^*_{p,t} \mid p \in \mathcal{P}, t \in \mathcal{T}\}$ with the PMFs $\{\boldsymbol{H}^{\tau+1}_{p,t} \mid \forall p \in \mathcal{P}, \forall t \in \mathcal{T}\}$, and then use the sample to generate the solution $\boldsymbol{Y}^*$ of **(SP2-E)**. Since **(SP2-E)** is equivalent to **(SP2)**, the solution of **(SP2)** is $z^*_{i,t,k} = y^*_{p,t,k}, \ \forall p \in \mathcal{P}, \forall t \in \mathcal{T}, \forall k \in \mathcal{C}_t, \forall i \in \mathcal{Q}_p$. Output $\boldsymbol{Z^*_t} = \{z^*_{i,t,k} \mid \forall i \in \mathcal{N}, \forall t \in \mathcal{T}, \forall k \in \mathcal{C}_t\}$.

Note that, the stopping rules of ECHA can guarantee the computational complexity within a controllable range. Meanwhile, the update of PMF in each iteration can make the generated samples toward better solutions.

6 JASC: Proposed Joint Channel Access and Sampling Rate Control Scheme

From the discussion of the previous subsections, we can efficiently solve the subproblems of the dual problem **(DP-NUMP)** with given $\boldsymbol{\alpha}$ and $\boldsymbol{\beta}$. In this section, we summarize the steps of solving **(NUMP)** by the subgradient method and propose a joint channel access and sampling rate control scheme, named JASC, to maximize the network utility.

6.1 Algorithm for Solving (NUMP)

We first focus on the primal problem **(NUMP)**, which is to schedule the channel access and sampling rates of sensor nodes over a period. According to the system model, except the decision variables $\boldsymbol{S}$ and $\boldsymbol{Z}$, all the parameters of **(NUMP)** are known in advance or can be predicted for the next T time slots, including the energy harvesting rate $\phi_{i,t}$, and the available channel set $\mathcal{C}_t$. **(NUMP)** can be solved by addressing its dual problem **(DP-NUMP)** with the subgradient method discussed in Section 4.3. Since there is a duality gap between **(NUMP)** and **(DP-NUMP)**, we introduce a duality gap threshold to terminate the iteration of solving **(DP-NUMP)**. Moreover, a maximum iteration number Π is predefined to guarantee the efficiency of the algorithm when the convergence is slow. Specifically, the main idea of solving **(NUMP)** is described in **Algorithm 1**.

This article has been accepted for publication in a future issue of this journal, but has not been fully edited. Content may change prior to final publication. Citation information: DOI 10.1109/TETC.2016.2555806, IEEE Transactions on Emerging Topics in Computing

Algorithm 1 Subgradient Method for Solving **(NUMP)**.

Input: The parameters of **(NUMP)**, the maximum iteration number Π and duality gap threshold δ.

Output: The optimal $\boldsymbol{S}^*$ and $\boldsymbol{Y}^*$.

1: Let $m = 1$; Initialize Lagrangian multipliers $\alpha_{i,t}(m) = 1$ and $\beta_{i,t}(m) = 1$;
2: **repeat**
3: With given $\boldsymbol{\alpha}(m)$ and $\boldsymbol{\beta}(m)$, determine the optimal $\boldsymbol{S}^*(m)$ and $\boldsymbol{Y}^*(m)$ by solving **(SP1)** and **(SP2)** according to **Proposition 1** and the CEHA in Section 5.3, respectively;
4: With the derived $\boldsymbol{S}^*(m)$ and $\boldsymbol{Y}^*(m)$, calculate the values of U and $D(\boldsymbol{\alpha}, \boldsymbol{\beta})$ as $U^*(m)$ and $D^*(\alpha(m), \beta(m))$, according to Eq. (9) and (15), respectively;
5: Generate $\boldsymbol{\alpha}^*(m+1)$ and $\boldsymbol{\beta}^*(m+1)$ for the next iteration according to Eq. (16);
6: $m = m + 1$;
7: **until** $D^*(\alpha(m), \beta(m)) - U^*(m) \leq \omega$ or $m > \Pi$;
8: **return** $\boldsymbol{S}^*(m)$ and $\boldsymbol{Y}^*(m)$;

6.2 Joint Channel Access and Sampling Rate Control Scheme

In **Algorithm 1**, the channel access and sampling rate control solution is determined based on the predicted energy harvesting rates and available channel sets over the whole period. Although existing prediction algorithms can achieve an acceptable accuracy, the prediction error, especially in the availability of licensed channels, cannot be entirely avoided and will impact the solution of **Algorithm 1**. For example, if channel k is wrongly predicted as available at time slot t and is scheduled to be accessed by the CRSN, the CRSN will suffer from significant interference caused by PUs. Therefore, to avoid such situation, the CRSN should communicate with the spectrum market to require the real-time available channel set $\mathcal{C}_t'$ at the beginning of each time slot t and use the real-time available set to adjust the channel access and sampling rate control solution.

To this end, we propose a joint channel access and sampling rate control scheme, named JASC, which can provide a real-time solution based on the real-time $\mathcal{C}_t'$ and energy harvesting rate $\phi_{i,t}'$ to maximize the network utility. Fig. 4 shows the main ideas of the JASC scheme and **Algorithm 2** presents the detailed procedures.

7 Performance Evaluation

In this section, we evaluate the performance of the proposed JASC scheme by extensive simulations on OMNET++ [34], [35]. We setup a network consisting of 8 sensor nodes and a sink node. The network topology is the same as Fig. 2. Each sensor node has a 30×30 mm^2 solar photovoltaic panel with an energy conversion efficiency 20%, and a rechargeable battery with enough capacity [12]. For example, if the solar radiation data during a time slot is 100 W/m^2, the

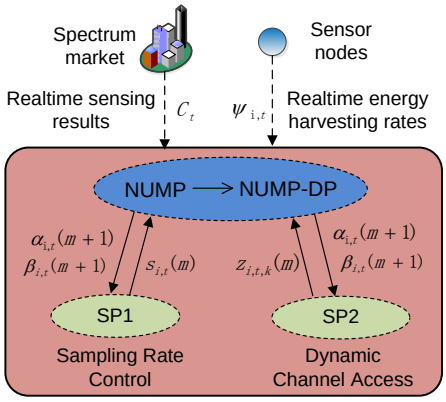

Fig. 4. Illustration of the JASC scheme.

Algorithm 2 Joint Channel Access and Sampling Rate Control Scheme (JASC).

Input: The inputs of Algorithm 1.

Output: The optimal sampling rates $\boldsymbol{S}_t'$ and channel access schedule $\boldsymbol{Y}_t'$ at each time slot t.

1: $t = 1$;
2: **repeat**
3: At the beginning of time slot t, communicate with the spectrum market to require the realistic available channel set $\mathcal{C}_t'$ and obtain the energy harvesting rates of sensor nodes $\{\psi_{1,t}', ..., \psi_{N,t}'\}$;
4: Use $\mathcal{C}_t'$ and $\psi_{i,t}'$, as well as the predicted available sets $\{\mathcal{C}_{t+1}, ..., \mathcal{C}_T\}$ and energy harvesting rates $\{\psi_{i,l} |\ 1 \leq i \leq N, t+1 \leq l \leq T\}$, as input to run **Algorithm 1** to obtain the real-time sampling rates $\boldsymbol{S}_t' = \{s_{1,t}', ..., s_{N,t}'\}$ and channel access schedule $\boldsymbol{Y}_t' = \{y_{i,t,k} \mid \forall i \in \mathcal{N}, \forall k \in \mathcal{C}_t'\}$ for time slot t;
5: Adjust the sampling rates and schedule the channel access of sensor nodes according to $\boldsymbol{S}_t'$ and $\boldsymbol{Y}_t'$;
6: $t = t + 1$;
7: **until** $t \geq T$;
8: **return** $\boldsymbol{S}_t'$ and $\boldsymbol{Y}_t'$ for each $t \in \mathcal{T}$;

corresponding energy harvesting rate is 0.018 J/s. The energy consumption rates for data sampling, receiving, and transmitting are 0.0013 J/Kb, 0.0024 J/Kb, and 0.0046 J/Kb, respectively, which are adopted from the measurements on the Mica 2 platform [36], [37]. The initial battery level is 0.05 J. The energy harvesting cycle is a day, and we divide each cycle into 24×6 time slots. Then, the duration of each time slot is 10 $mins$. Meanwhile, there are 10 licensed channels in the primary network. The capacity of the m-th ($1 \leq m \leq 10$) licensed channel is $5 * m$ Kb/s, and the idle probability of each licensed channel is 65%, and the channel cost φ is 0.02. The main parameter settings are summarized in Table 2.

The energy harvesting rates of sensor nodes are set according to the real solar data collected by the NREL Solar Radiation Research Laboratory in Rancho Cordova, California [38]. We choose the solar radiation data on

This article has been accepted for publication in a future issue of this journal, but has not been fully edited. Content may change prior to final publication. Citation information: DOI 10.1109/TETC.2016.2555806, IEEE Transactions on Emerging Topics in Computing

TABLE 2
Parameter Settings

Parameters	Settings	Parameters	Settings
e_s	$0.0013\ J/Kb$	e_r	$0.0024\ J/Kb$
e_t	$0.0046\ J/Kb$	Δt	$300\ s$
$\|\mathcal{N}\|$	8	$\|\mathcal{T}\|$	288
$r_{i,0}$	$0.05\ J$	e_w	$10^{-4}\ J$
C_m	$5 * m\ Kb/s$	m	$[1, ..., 10]$

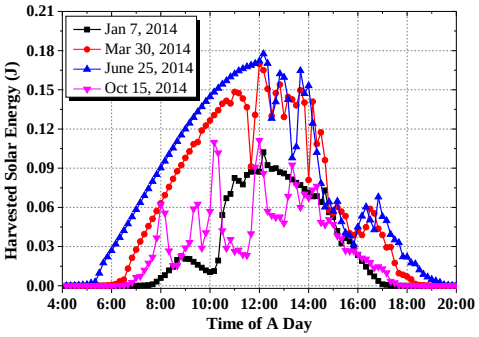

Fig. 5. Energy Harvesting Rates on Different Days.

four different days, which can provide different amount of solar energy for sensor nodes, to generate the energy harvesting profiles. The energy harvesting rates of a sensor node in the four days are shown in Fig. 5. To evaluate the effectiveness of JASC, we compare it with an existing method, named DSCC [12]. Since DSCC is proposed for sampling rate control in traditional rechargeable sensor networks, we employ a dynamic channel allocation algorithm named GBCA [39], to collaborate with DSCC for sampling rate and channel access control in cognitive radio sensor networks. We first dynamically allocate the available licensed channels to sensor nodes by GBCA, and then use DSCC to schedule the sampling rates of sensor nodes for network utility maximization.

7.1 Utility Comparison and Efficiency Evaluation

Fig. 6 shows the network utility comparison on different days. It can be seen from the figure that JASC can achieve improved network utility than DSCC+GBCA on different days. The improved ratio is close to 10%. Especially, when the harvested solar energy is plentiful, e.g. on June 25, 2014, the improved ratio is approaching 15%. Fig. 7 shows the network utility comparison under different network scales. It can be seen that JASC can outperform DSCC+GBCA under different network scales, in terms of network utility. Moreover, with the increasing number of sensor nodes, the network utility of both schemes gradually increases. However, it experiences very slight increment after the number of sensor nodes achieves 40. This is because the limited network capacity will significantly decrease the sampling rates of sensor nodes under a large network scale.

Fig. 8 shows the converge speed comparison of JASC

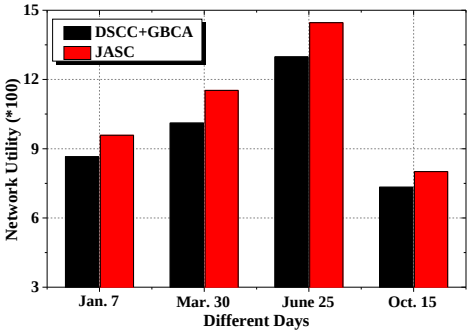

Fig. 6. Network Utility Comparison on Different Days.

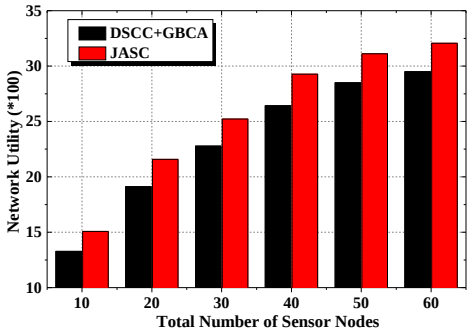

Fig. 7. Network Utility Comparison under Different Network Scales.

under different network scales. As shown in the figure, the network utility of JASC can quickly converge to a certain value within 20 iterations, when there are 8 sensor nodes in the network. But when the network scale increases to 20 sensor nodes, JASC has to experience nearly 50 iterations to achieve a converged network utility. Although the increasing network scale can degrade the converge speed of JASC, JASC still has a high efficiency to achieve a converged network utility.

7.2 Channel Access and Interference Evaluation

In this subsection, we aim to evaluate the dynamic channel access of sensor nodes and channel interference probability of JASC. Fig. 9 shows the accessed channels

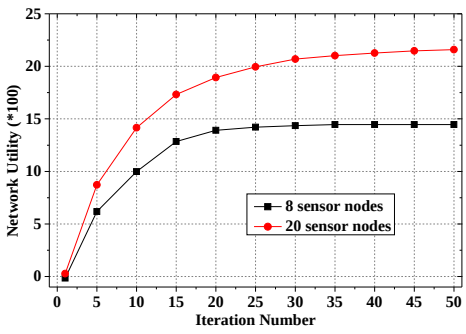

Fig. 8. Converge Speed Comparison of JASC under Different Network Scales.

This article has been accepted for publication in a future issue of this journal, but has not been fully edited. Content may change prior to final publication. Citation information: DOI 10.1109/TETC.2016.2555806, IEEE Transactions on Emerging Topics in Computing

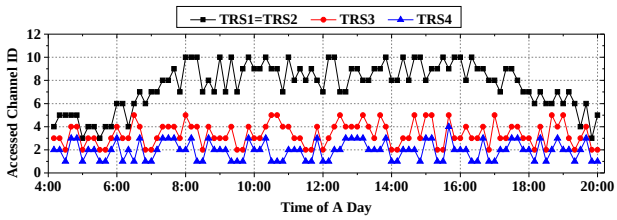

Fig. 9. Accessed Channels over Different Time Slots.

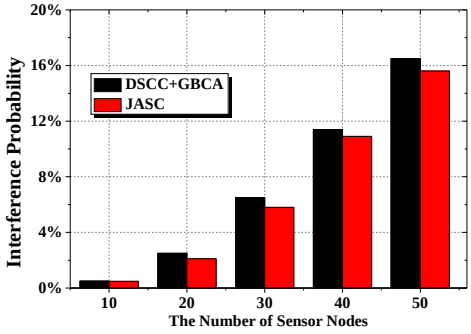

Fig. 10. Channel Interference Comparison under Different Network Scales.

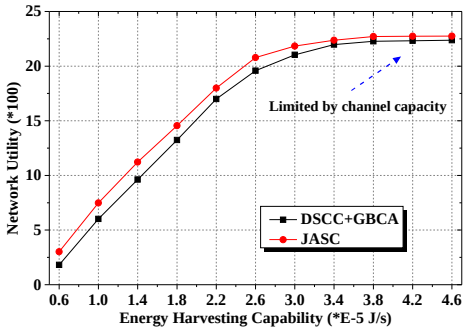

Fig. 11. Impacts of Energy Harvesting Capability on Network Utility.

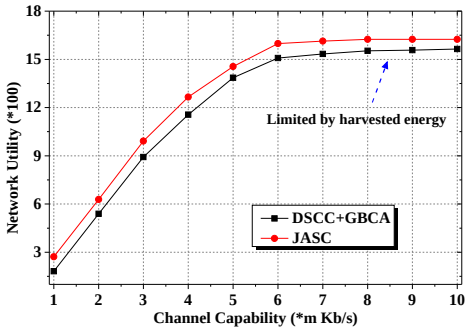

Fig. 12. Impacts of Channel Capacity on Network Utility.

of different sensor nodes over different time slots under the network topology (i.e., Fig. 2). It can be seen that the sensor nodes in TRS1 and TRS2 keep accessing the same channel due to no interference between them, while the sensor nodes in TRS3 and TRS4 access different channels with lower bandwidth. Since TRS1 is the bottleneck of the whole network capacity, it can greatly increase the network capacity by accessing a channel with large bandwidth. However, since the harvested energy is another key factor to limit the network throughput, TRS1 choose to access the channels with low bandwidth to save channel cost when the time is before 8:00am and after 18:00. Because during those time slots, the harvested energy can only afford a low network throughput, which can be guaranteed by accessing the channels with low bandwidth. Furthermore, the stochastic channel availability makes the accessed channel of each TRS vary over different time slots.

We also compare JASC with DSCC+GBCA under different network scenarios in Fig. 10, in terms of channel interference probability. It can be observed that the channel interference probability increases with the number of sensor nodes under a certain number of licensed channels. This is because a larger number of sensor nodes may produce a more complicated TRS partition, which requires more available channels to avoid interference. When the number of channels is fixed, interference probability may increase with the required number of available channels.

7.3 Impacts of System Parameters

In this subsection, we evaluate the impacts of two system parameters, including energy harvesting capability and channel capacity, on the performance of JASC.

Fig. 11 shows the impacts of energy harvesting capability on network utility. The energy harvesting capability in this figure is defined as the energy harvesting rate of a sensor node when the solar radiation is $1W/m^2$. It can be observed that network utility increases with energy harvesting capability under both of JASC and DSCC+GBCA. However, it does not increase indefinitely but reaches the saturation points, which are caused by the limited channel capacity, after the energy harvesting capability becomes larger than $3.8 * 10^{-5} J/s$. Fig. 12 shows the impacts of channel capacity on network utility. The channel capacity here is defined as the channel capacity of channel 1. It means that, for each channel $1 \leq m \leq 10$, its channel capacity is $m * dKb/s$, where d is the defined channel capacity in the figure. Similar to the situation in Fig. 11, network utility keeps pace with the growing channel capacity and achieves its saturation point when the channel capacity is over $7Kb/s$, due to the limited harvested energy.

8 Conclusion

In this paper, we have investigated the network utility maximization problem in energy harvesting CRSNs by jointly considering the sampling rate control and dynamic channel access. We have formulated the problem

as a mix-integer non-linear programming problem. By employing dual decomposition, the joint optimization problem is decoupled as two separable subproblems. We have also proposed a joint channel access and sampling rate control scheme, named JASC, for utilizing the real-time sensing results to adjust the dynamic channel access and sampling rates for sensor nods. Simulation results demonstrate that the proposed JASC can achieve an improved network utility than existing methods. For our future work, we will study CRSNs with dynamic routing, where the channel access and sampling rate control should be adaptive to the dynamically changed routing paths.

REFERENCES

[1] J. Ren, Y. Zhang, K. Zhang, and X. Shen, "Sacrm: Social aware crowdsourcing with reputation management in mobile sensing," *Comput. Commun.*, vol. 65, no. 15, pp. 55–65, 2015.

[2] Z. Su, Q. Xu, and Q. Qi, "Big data in mobile social networks: a qoe-oriented framework," *IEEE Netw.*, vol. 30, no. 1, pp. 52–57, 2016.

[3] C. Huang, R. Zhang, and S. Cui, "Throughput maximization for the gaussian relay channel with energy harvesting constraints," *IEEE J. Selected Areas Commun.*, vol. 31, no. 8, pp. 1469–1479, 2013.

[4] N. Zhang, H. Liang, N. Cheng, Y. Tang, J. W. Mark, and X. Shen, "Dynamic spectrum access in multi-channel cognitive radio networks," *IEEE J. Selected Areas Commun.*, vol. 32, no. 11, pp. 2053–2064, 2014.

[5] Z. Liang, S. Feng, D. Zhao, and X. Shen, "Delay performance analysis for supporting real-time traffic in a cognitive radio sensor network," *IEEE Trans. Wirel. Commun.*, vol. 10, no. 1, pp. 325–335, 2011.

[6] A. O. Bicen, V. C. Gungor, and O. B. Akan, "Delay-sensitive and multimedia communication in cognitive radio sensor networks," *Ad Hoc Netw.*, vol. 10, no. 5, pp. 816–830, 2012.

[7] S.-C. Lin and K.-C. Chen, "Improving spectrum efficiency via in-network computations in cognitive radio sensor networks," *IEEE Trans. Wirel. Commun.*, vol. 13, no. 3, pp. 1222–1234, 2014.

[8] J. Liu, J. Gao, X. Jiang, H. Nishiyama, and N. Kato, "Capacity and delay of probing-based two-hop relay in manets," *IEEE Trans. Wirel. Commun.*, vol. 11, no. 11, pp. 4172–4183, 2012.

[9] P. T. A. Quang and D.-S. Kim, "Throughput-aware routing for industrial sensor networks: Application to isa100. 11a," *IEEE Trans. Industrial Info.*, vol. 10, no. 1, pp. 351–363, 2014.

[10] P. Spachos and D. Hantzinakos, "Scalable dynamic routing protocol for cognitive radio sensor networks," *IEEE Sensors J.*, vol. 14, no. 7, pp. 2257–2266, 2014.

[11] R.-S. Liu, P. Sinha, and C. E. Koksal, "Joint energy management and resource allocation in rechargeable sensor networks," in *IEEE Proc. INFOCOM*, 2010, pp. 1–9.

[12] R. Deng, Y. Zhang, S. He, J. Chen, and X. Shen, "Maximizing network utility of rechargeable sensor networks with spatiotemporally-coupled constraints," *IEEE J. Selected Areas Commun.*, 2016, DOI: 10.1109/JSAC.2016.2520181, to appear.

[13] S. Chen, P. Sinha, N. B. Shroff, and C. Joo, "A simple asymptotically optimal joint energy allocation and routing scheme in rechargeable sensor networks," *IEEE/ACM Trans. Netw.*, vol. 22, no. 4, pp. 1325–1336, 2014.

[14] L. Huang and M. J. Neely, "Utility optimal scheduling in energy-harvesting networks," *IEEE/ACM Trans. Netw.*, vol. 21, no. 4, pp. 1117–1130, 2013.

[15] Z. Mao, C. E. Koksal, and N. B. Shroff, "Near optimal power and rate control of multi-hop sensor networks with energy replenishment: Basic limitations with finite energy and data storage," *IEEE Trans. Auto. Cont.*, vol. 57, no. 4, pp. 815–829, 2012.

[16] Y. Zhang, S. He, J. Chen, Y. Sun, and X. Shen, "Distributed sampling rate control for rechargeable sensor nodes with limited battery capacity," *IEEE Trans. Wirel. Commun.*, vol. 12, no. 6, pp. 3096–3106, 2013.

[17] C. Huang, R. Zhang, and S. Cui, "Optimal power allocation for outage probability minimization in fading channels with energy harvesting constraints," *IEEE Trans. Wirel. Commun.*, vol. 13, no. 2, pp. 1074–1087, 2014.

[18] J. A. Han, W. S. Jeon, and D. G. Jeong, "Energy-efficient channel management scheme for cognitive radio sensor networks," *IEEE Trans. Veh. Tech.*, vol. 60, no. 4, pp. 1905–1910, 2011.

[19] G. A. Shah and O. B. Akan, "Performance analysis of csma-based opportunistic medium access protocol in cognitive radio sensor networks," *Ad Hoc Netw.*, vol. 15, pp. 4–13, 2014.

[20] G. Shah and O. Akan, "Cognitive adaptive medium access control in cognitive radio sensor networks," *IEEE Trans. Veh. Tech.*, vol. 64, no. 2, pp. 757–767, 2015.

[21] J. Ren, Y. Zhang, N. Zhang, D. Zhang, and X. Shen, "Dynamic channel access to improve energy efficiency in cognitive radio sensor networks," *IEEE Trans. Wirel. Commun.*, DOI: 10.1109/TWC.2016.2517618, to appear.

[22] G. A. Shah, F. Alagoz, E. A. Fadel, and O. B. Akan, "A spectrum-aware clustering for efficient multimedia routing in cognitive radio sensor networks," *IEEE Trans. Veh. Tech.*, vol. 63, no. 7, pp. 3369–3380, 2014.

[23] M. Ozger and O. Akan, "Event-driven spectrum-aware clustering in cognitive radio sensor networks," in *IEEE Proc. INFOCOM*, 2013, pp. 1483–1491.

[24] X. Xing, T. Jing, W. Cheng, Y. Huo, and X. Cheng, "Spectrum prediction in cognitive radio networks," *IEEE Wireless Commun.*, vol. 20, no. 2, pp. 90–96, 2013.

[25] V. K. Tumuluru, P. Wang, and D. Niyato, "A neural network based spectrum prediction scheme for cognitive radio," in *IEEE Proc. ICC*, 2010, pp. 1–5.

[26] J. Liu and N. Kato, "Device-to-device communication overlaying two-hop multi-channel uplink cellular networks," in *Proc. ACM MobiHoc*, 2015, pp. 307–316.

[27] M. Guzelsoy, *Dual methods in mixed integer linear programming*. Lehigh University, 2009.

[28] I. Nowak, *Relaxation and decomposition methods for mixed integer nonlinear programming*. Springer Science & Business Media, 2006, vol. 152.

[29] S. Boyd and L. Vandenberghe, *Convex optimization*. Cambridge university press, 2004.

[30] R. Deng, G. Xiao, R. Lu, and J. Chen, "Fast distributed demand response with spatially and temporally coupled constraints in smart grid," *IEEE Trans. Ind. Info.*, vol. 11, no. 6, pp. 1597–1606, 2015.

[31] K. R. Duffy, N. O'Connell, and A. Sapozhnikov, "Complexity analysis of a decentralised graph colouring algorithm," *Information Processing Letters*, vol. 107, no. 2, pp. 60–63, 2008.

[32] T. R. Jensen and B. Toft, *Graph coloring problems*. John Wiley & Sons, 2011.

[33] P.-T. De Boer, D. P. Kroese, S. Mannor, and R. Y. Rubinstein, "A tutorial on the cross-entropy method," *Annals of operations research*, vol. 134, no. 1, pp. 19–67, 2005.

[34] J. Ren, Y. Zhang, K. Zhang, A. Liu, J. Chen, and X. Shen, "Lifetime and energy hole evolution analysis in data-gathering wireless sensor networks," *IEEE Trans. Industrial Info.*, vol. 12, no. 2, pp. 788–800, 2016.

[35] J. Ren, Y. Zhang, K. Zhang, and X. Shen, "Adaptive and channel-aware detection of selective forwarding attacks in wireless sensor networks," *IEEE Trans. Wirel. Commun.*, DOI: 10.1109/TWC.2016.2526601, to appear.

[36] M. Calle, "Energy consumption in wireless sensor networks using gsp," Master's thesis, University of Pittsburgh, Pittsburgh, 2006.

[37] J. Polastre, J. Hill, and D. Culler, "Versatile low power media access for wireless sensor networks," in *Proc. ACM SenSys*, 2004, pp. 95–107.

[38] Nrel: Midc/srrl baseline measurement system (39.74 n, 105.18 w, 1829 m, gmt-7). [Online]. Available: http://www.nrel.gov/midc/srrl_bms/

[39] J. Chen, Q. Yu, P. Cheng, Y. Sun, Y. Fan, and X. Shen, "Game theoretical approach for channel allocation in wireless sensor and actuator networks," *IEEE Trans. Auto. Cont.*, vol. 56, no. 10, pp. 2332–2344, 2011.

This article has been accepted for publication in a future issue of this journal, but has not been fully edited. Content may change prior to final publication. Citation information: DOI 10.1109/TETC.2016.2555806, IEEE Transactions on Emerging Topics in Computing

Ju Ren [S'13] (ren_ju@csu.edu.cn) received his B.Sc. and M.Sc. degrees in computer science from Central South University, China, in 2009 and 2012, respectively. He is currently a Ph.D. candidate in computer science at Central South University, China. From Aug. 2013 to Sept. 2015, he was also a visiting Ph.D. student in electrical and computer engineering at University of Waterloo, Canada. His research interests include wireless sensor network, mobile sensing/computing, and cloud computing.

Yaoxue Zhang (zyx@csu.edu.cn) received his B.S. degree from Northwest Institute of Telecommunication Engineering, China, in 1982, and his Ph.D. degree in computer networking from Tohoku University, Japan, in 1989. Currently, he is a professor in the Department of Computer Science at Central South University, China, and also a professor in the Department of Computer Science and Technology at Tsinghua University, China. His research interests include computer networking, operating systems, ubiquitous/pervasive computing, transparent computing, and big data. He has published over 200 technical papers in international journals and conferences, as well as 9 monographs and textbooks. He is a fellow of the Chinese Academy of Engineering and the president of Central South University, China.

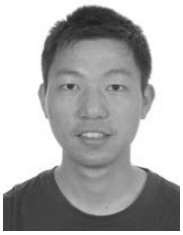

Ruilong Deng [S'11, M'14] (ruilong@ualberta.ca) received the B.Sc. and Ph.D. degrees both in Control Science and Engineering from Zhejiang University, China, in 2009 and 2014, respectively. He was a Visiting Scholar at Simula Research Laboratory, Norway, in 2011, and the University of Waterloo, Canada, from 2012 to 2013. He was a Research Fellow at Nanyang Technological University, Singapore, from 2014 to 2015. Currently, he is an AITF Postdoctoral Fellow with the Department of Electrical and Computer Engineering, University of Alberta, Canada. His research interests include smart grid, cognitive radio, and wireless sensor network. Dr. Deng currently serves as an Editor for IEEE/KICS Journal of Communications and Networks, and a Guest Editor for IEEE Transactions on Emerging Topics in Computing. He also serves/served as a Technical Program Committee Member for IEEE Globecom, IEEE ICC, IEEE SmartGridComm, EAI SGSC, etc.

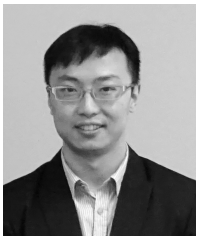

Ning Zhang [S'12] (n35zhang@uwaterloo.ca) earned the Ph.D degree from University of Waterloo in 2015. He received his B.Sc. degree from Beijing Jiaotong University and the M.Sc. degree from Beijing University of Posts and Telecommunications, Beijing, China, in 2007 and 2010, respectively. He is now a postdoc research fellow at BBCR lab in University of Waterloo. His current research interests include next generation wireless networks, software defined networking, green communication, and physical layer security.

Deyu Zhang (zdy876@csu.edu.cn) received his B.Sc. degree from the PLA Information Engineering University, Zhengzhou, China, in 2009, and his M.Sc. degree from Central South University, Changsha, China, in 2012. He is currently working towards the Ph.D. degree at Cetral South University, Changsha, China. From Aug. 2014 to Feb. 2015, he was also a visiting Ph.D. student in the Department of Electrical and Computer Engineering, University of Waterloo, Canada. His current research interests include wireless sensor networks and cognitive radio.

Xuemin (Sherman) Shen [M'97, SM'02, F'09] (xshen@bbcr.uwaterloo.ca) received the B.Sc.(1982) degree from Dalian Maritime University (China) and the M.Sc. (1987) and Ph.D. degrees (1990) from Rutgers University, New Jersey (USA), all in electrical engineering. He is a Professor and University Research Chair, Department of Electrical and Computer Engineering, University of Waterloo, Canada. He is also the Associate Chair for Graduate Studies. Dr. Shens research focuses on resource management in interconnected wireless/wired networks, wireless network security, social networks, smart grid, and vehicular ad hoc and sensor networks. He is an elected member of IEEE ComSoc Board of Governor, and the Chair of Distinguished Lecturers Selection Committee. Dr. Shen served as the Technical Program Committee Chair/Co-Chair for IEEE Globecom16, Infocom14, IEEE VTC10 Fall, and Globecom07, the Symposia Chair for IEEE ICC10, the Tutorial Chair for IEEE VTC'11 Spring and IEEE ICC08, the General Co-Chair for ACM Mobihoc15, Chinacom07 and QShine06, the Chair for IEEE Communications Society Technical Committee on Wireless Communications, and P2P Communications and Networking. He also serves/served as the Editor-in-Chief for IEEE Network, Peer-to-Peer Networking and Application, and IET Communications; a Founding Area Editor for IEEE Transactions on Wireless Communications; an Associate Editor for IEEE Transactions on Vehicular Technology, Computer Networks, and ACM/Wireless Networks, etc.; and the Guest Editor for IEEE JSAC, IEEE Wireless Communications, IEEE Communications Magazine, and ACM Mobile Networks and Applications, etc. Dr. Shen received the Excellent Graduate Supervision Award in 2006, and the Outstanding Performance Award in 2004, 2007, 2010, and 2014 from the University of Waterloo, the Premiers Research Excellence Award (PREA) in 2003 from the Province of Ontario, Canada, and the Distinguished Performance Award in 2002 and 2007 from the Faculty of Engineering, University of Waterloo. Dr. Shen is a registered Professional Engineer of Ontario, Canada, an IEEE Fellow, an Engineering Institute of Canada Fellow, a Canadian Academy of Engineering Fellow, a Royal Society of Canada Fellow, and a Distinguished Lecturer of IEEE Vehicular Technology Society and Communications Society.